



Luminescence properties of cyclometalated platinum(II) complexes in a dichloromethane/*n*-hexane system

Weitong Tao¹, Yan Chen¹, Lu Lu, Chun Liu*

State Key Laboratory of Fine Chemicals, Dalian University of Technology, Linggong Road 2, Dalian 116024, China



ARTICLE INFO

Article history:

Received 15 November 2020

Revised 18 December 2020

Accepted 21 December 2020

Available online 12 January 2021

Keywords:

Platinum(II) complexes

Aggregation-induced phosphorescent emission

Hydrogen bonding

Nanoaggregates

ABSTRACT

The luminescence properties of three neutral cyclometalated Pt(II) complexes were investigated in a CH₂Cl₂/*n*-hexane system. The diphenylamino and trifluoromethyl modified **Pt2** exhibits aggregation-induced phosphorescent emission (AIPE) feature. The crystal stacking of **Pt2** shows that the intermolecular hydrogen bonding restricts both intramolecular rotation (RIR) and vibration (RIV), which weakens the non-radiative decay ways and leads to an AIPE performance. TEM images reveal that **Pt2** aggregates into nanosheets.

© 2021 Elsevier Ltd. All rights reserved.

Introduction

Platinum(II) complexes are sensitive upon external stimuli on account of their square planar geometry and conjugated ligand structure, which are generally influenced by intra- and intermolecular Pt...Pt and/or π - π stacking interactions [1–6]. Pt(II) complexes exhibit rich spectroscopic and luminescence properties such as high luminescence quantum yields, long emission lifetimes, large Stoke shifts and color tunability [7–11]. Therefore, Pt(II) complexes have been used as promising candidates for applications in organic light-emitting devices (OLEDs) [12–15], bio-imaging [16–18], drug discovery [19–23], and so on. In the past years, most of the traditional organic luminescent materials are well known to suffer from aggregation-caused quenching (ACQ) in the solid state [24,25], which has greatly restricted the applications of organic luminescent materials in many fields. In 2001, Tang and co-workers [26] reported that a silole derivative was almost non-emissive in dilute solution but strongly emissive in aggregated state. Aggregation-induced emission (AIE) has settled a great deal of problems with ACQ fundamentally, and has attracted attention as a new approach for the development of novel optoelectronic materials [27–31].

It is well known that the hydrogen bonds, including C–H...N, C–H...O and C–H...F, contribute to the photophysical behaviors of the dyes. Although individual hydrogen bonding is relatively weak, multiple hydrogen bonding array may show much stronger

binding strength and offer the molecules high stability [32]. Honda et al. [33] discovered that a thioamide-based cationic pincer Pt(II) complex was AIE-active induced by hydrogen bonding (N–H...Cl[−]) in the absence of traditional Pt...Pt interaction. Kuwabara et al. [34] reported that a cationic Pt(II) complex exhibited three emission modes: blue (monomer emission), yellow (hydrogen-bonded dimer) and orange (aggregate emission), which was modulated by a combination of hydrogen bonding (N–H...Cl[−]) and a solvophobic effect. Yang et al. [13] synthesized a neutral fluorine-substituted Pt(II) complex, whose photophysical properties, molecular packing orientation and electron transport ability were tuned through C–H...F hydrogen bonding. The previous discoveries show that the number and the type of hydrogen bonding play an important role in adjusting the performances of luminescent materials.

We have a long-term interest in disclosing the relationship between the molecular structures of the cyclometalated metal complexes and their properties [35–39]. Herein, three neutral Pt(II) complexes (Scheme 1) were synthesized using acetylacetone as the ancillary ligand and their luminescence properties were investigated in a CH₂Cl₂/*n*-hexane system in detail to study the effects of the intermolecular hydrogen bonding on the properties.

Results and discussion

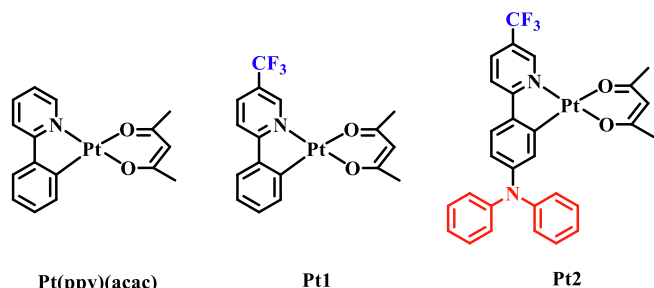
Molecular design

The chemical structures of platinum(II) complexes are shown in Scheme 1. Using Pt(ppy)(acac) as a reference, a trifluoromethyl

* Corresponding author.

E-mail address: cliu@dlut.edu.cn (C. Liu).

¹ These authors contributed equally to this work.



Scheme 1. Chemical structures of Pt(II) complexes for this study.

(TFM) group was introduced onto **Pt1** to construct intermolecular hydrogen bonding. Both a TFM group and a rotatable diphenylamino (DPA) moiety were introduced into the cyclometalating ligand of **Pt2** to reach different luminescence properties compared to Pt(ppy)(acac) and **Pt1**.

Luminescence properties

To study the luminescence properties of all complexes, the emission spectra were investigated in a CH₂Cl₂/*n*-hexane system with different volume ratios. As depicted in Fig. 1, Pt(ppy)(acac), **Pt1** and **Pt2** exhibit different emission profiles with the increase of *n*-hexane in the mixed solvent. The phosphorescence emission intensity of Pt(ppy)(acac) decreases dramatically as the *n*-hexane fraction increases, which shows an obvious ACQ phenomenon (Fig. 1A). Nevertheless, the phosphorescence emission intensity

of **Pt1** has a slight enhancement with the addition of *n*-hexane, but decreases apparently when the *n*-hexane fraction increases to 90%, which shows an inconspicuous AIPE property. However, the **Pt2** demonstrates a typical AIPE feature in the CH₂Cl₂/*n*-hexane system. As shown in Fig. 1C, the phosphorescence emission intensity of **Pt2** increases steadily when the *f*_{*n*-Hexane} is less than 60%, whereas the intensity is enhanced sharply when increasing the *n*-hexane fraction from 60% to 90% and then reaches the maximum at 90% *n*-hexane fraction. Fig. 1D shows a stable emission intensity of **Pt2** over time at the 90% *n*-hexane content in the CH₂Cl₂/*n*-hexane system, which means that the aggregation process goes to the equilibrium quickly.

Molecular packing mode

In order to clarify the relationship between the intermolecular interaction of **Pt1** and **Pt2** and their luminescence properties, the multiple intermolecular interactions of **Pt1** and **Pt2** were studied in detail by analyzing molecular packing of their crystal structures, respectively. The single crystals were cultivated by slowly evaporating the solvents from a CHCl₃/cyclohexane system and fully investigated by single-crystal X-ray diffraction analysis. The crystal analysis figures and corresponding data for **Pt1** and **Pt2** are illustrated in Figs. 2–4 and Tables S2–S4.

As shown in Fig. 2, **Pt1** molecules pack as antiparallel dimers in crystals and possess Pt...Pt interactions with a 3.90 Å mean distance (Fig. 2, Table S3). Because of this special packing arrangement, abundant intermolecular hydrogen bonds could be observed in the crystal structures. As shown in Fig. 2B, C—H...N, C—H...O and C—H...F hydrogen bonds were found in the molecular

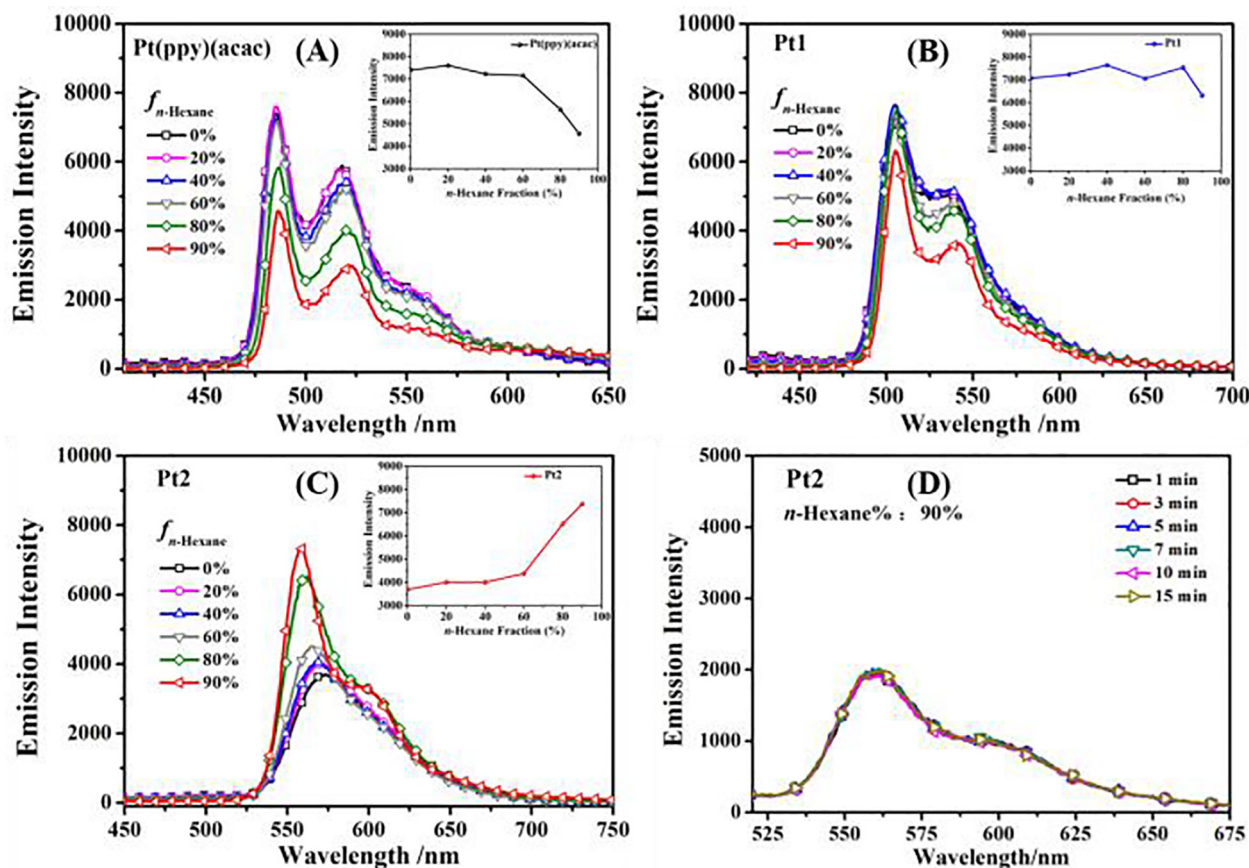


Fig. 1. Emission spectra of Pt(ppy)(acac) (A), **Pt1** (B) and **Pt2** (C) (5.0×10^{-5} mol L⁻¹) in CH₂Cl₂/*n*-hexane with different *n*-hexane fraction (0–90%) at room temperature. Emission spectra (D) of **Pt2** (5.0×10^{-5} mol L⁻¹) over time with a 90% *n*-hexane fraction at room temperature.

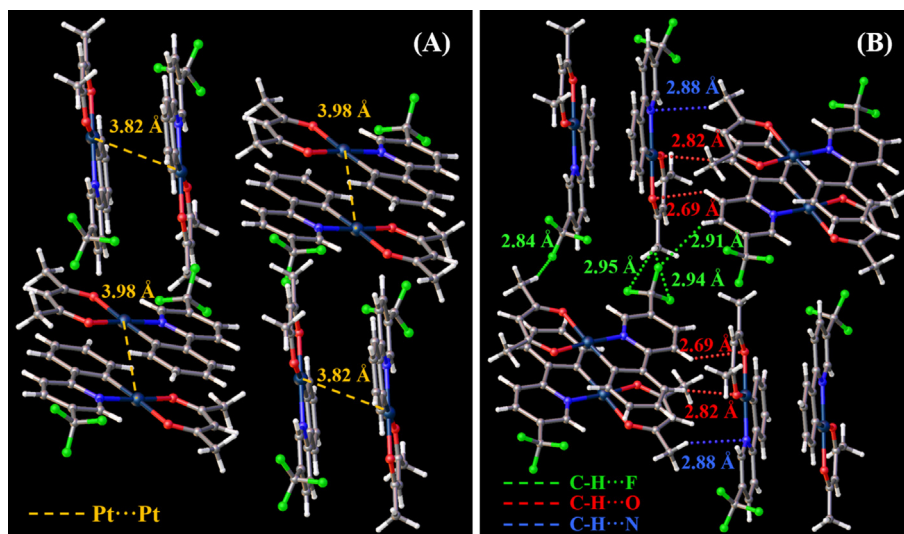


Fig. 2. Molecular packing of **Pt1** in crystal state. The orange dashed lines (A) represent the Pt...Pt interactions. The green, red and blue dashed lines (B) represent the C—H...F, C—H...O and C—H...N hydrogen bonding, respectively.

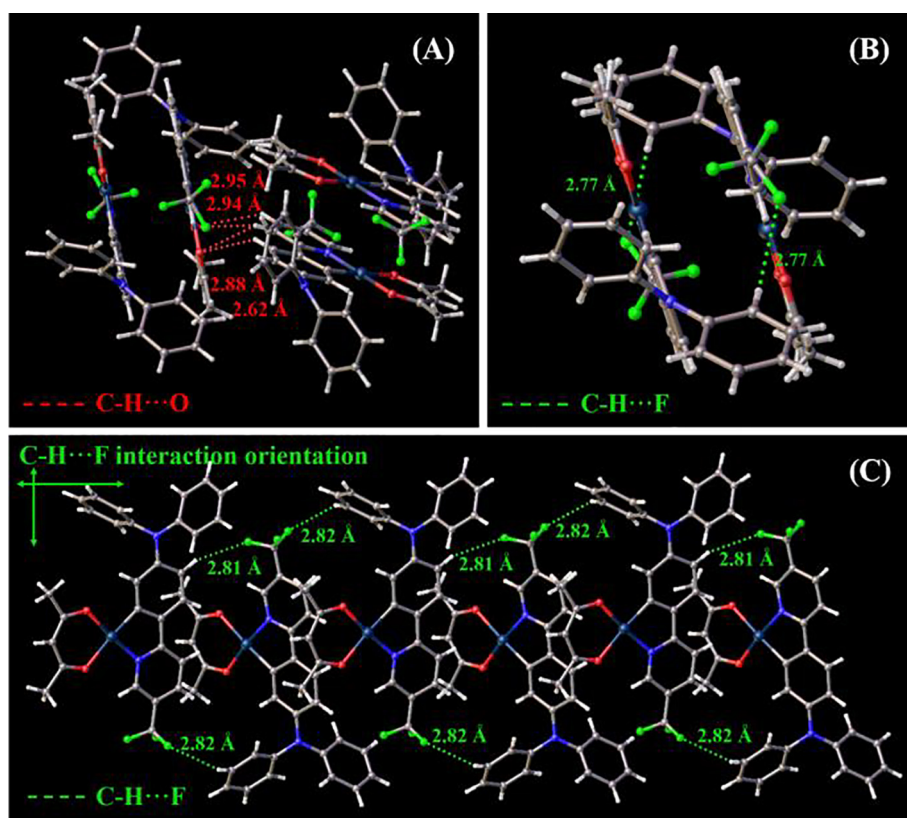


Fig. 3. Molecular packing of **Pt2** in crystal state. The red (A) and green (B, C) represent the C—H...O and C—H...F hydrogen bonding, respectively.

packing of **Pt1**. The C—H...O hydrogen bonding exists between the acetylacetonate (acac) ligand of one molecule and the 2-phenylpyridine moiety of the neighboring molecule (Fig. 2B). The presence of C—H...F hydrogen bonding could be found among the F atoms of one molecule's TFM group and the H atoms of two other molecules in different dimers, which plays an important role in restricting the intramolecular vibration (RIV) effectively (Fig. 2B) [40–42]. Therefore, these intermolecular interactions cause a more rigid

molecular environment to suppress the non-radiative pathways, leading to an AIPE performance.

As shown in Figs. 3 and 4, the molecular packing of **Pt2** also shows a plane stacking with antiparallel dimers. This arrangement allows the formation of C—H...O hydrogen bonding between the H atoms of 2-phenylpyridine and the O atoms at acetylacetonate of the neighboring molecule (Fig. 3A). Meanwhile, the intermolecular C—H...F hydrogen bonding (2.77 Å) is found in dimers (Fig. 3B,

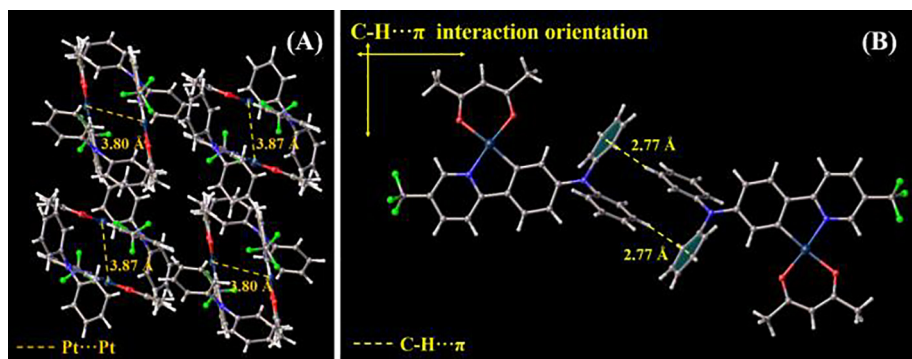


Fig. 4. Molecular packing of **Pt2** in crystal state. The orange dashed lines (A) represent the Pt...Pt interactions. The yellow dashed lines (B) represent the C—H... π intermolecular interactions.

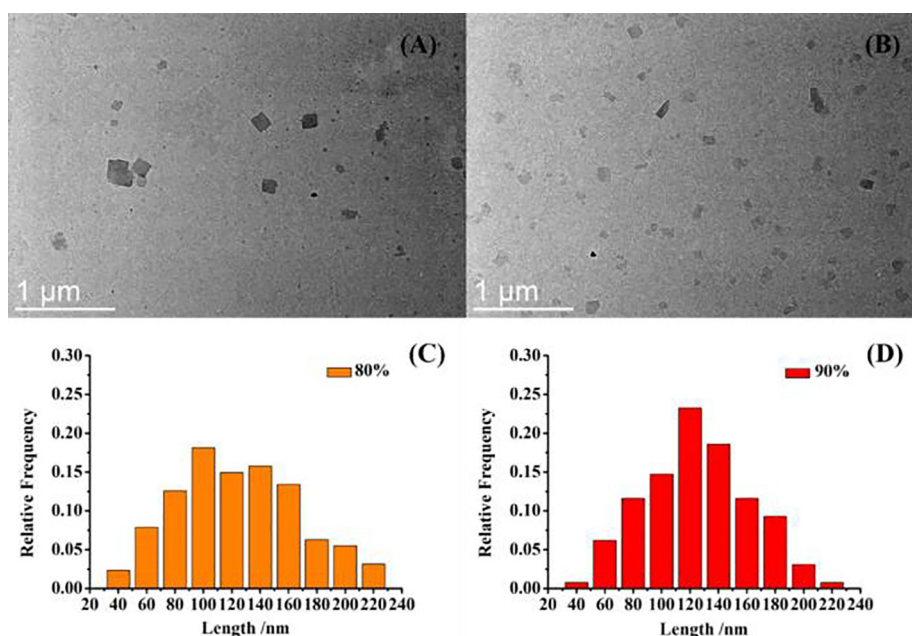


Fig. 5. TEM images of **Pt2** in $\text{CH}_2\text{Cl}_2/n$ -hexane ($5.0 \times 10^{-5} \text{ mol L}^{-1}$) with 80% (A) and 90% (B) n -hexane fraction at room temperature (after deoxygenated). The distribution charts of the length of nanosheets with 80% (C) and 90% (D) n -hexane fraction for **Pt2** aggregates.

Table S4) between the F atoms of TFM and the H atoms of phenyl group at the DPA moiety. It is worth noting that this molecular packing mode results in the netlike formation of C—H...F hydrogen bonding between the obliquely molecule in adjacent dimers of **Pt2**, which restricts the rotation of the phenyl groups at the DPA moiety greatly (Fig. 3C).

Compared to **Pt1**, **Pt2** molecules pack much denser due to the stronger intermolecular Pt...Pt interaction with a mean distance of 3.83 Å (Fig. 4A, Table S3). In addition, the adjacent **Pt2** molecules in opposite direction are interlocked by symmetric C—H... π intermolecular interactions (2.77 Å) between the phenyl groups of DPA (Fig. 4B). In the aggregated state, the synergistic effect of these multiple intermolecular interactions contributes to a rigid molecular environment to restrict non-radiative process [40]. Thus, **Pt2** demonstrates an obvious AIPE property in the $\text{CH}_2\text{Cl}_2/n$ -hexane system.

Thus, the intramolecular vibration of **Pt1** is limited by a combination of Pt...Pt interaction and intermolecular hydrogen bonding. In case of **Pt2**, the much more abundant intermolecular interactions caused by the DPA moiety result in the restriction of intramolecular vibration (RIV) and intramolecular rotation (RIR)

[43–45], leading to a more remarkable AIPE property. On the other hand, the multiple intermolecular interactions could explain the fast aggregation of **Pt2** at the 90% n -hexane content (Fig. 1D).

Aggregate morphology

To further investigate the formation of aggregates, transmission electron micrograph (TEM) images of the aggregate morphology of **Pt2** in $\text{CH}_2\text{Cl}_2/n$ -hexane ($5.0 \times 10^{-5} \text{ mol L}^{-1}$) with 80% and 90% n -hexane fractions are shown in Fig. 5. The aggregates of **Pt2** are regular square nanosheets with different sizes (Fig. 5A, B). The aggregates (100–120 nm, Fig. 5C) formed at an 80% n -hexane fraction are little smaller than those (120–140 nm, Fig. 5D) at a 90% n -hexane fraction.

Conclusion

In conclusion, three neutral cyclometalated Pt(II) complexes with different luminescence properties have been reported. **Pt2** performs a typical AIPE feature in the $\text{CH}_2\text{Cl}_2/n$ -hexane system,

while Pt(ppy)(acac) exhibits an obvious ACQ phenomenon. The TFM-modified **Pt1** displays feeble AIPE property. The crystal stacking exhibits that the combination of abundant intermolecular hydrogen bonding and Pt...Pt interactions restricts the intramolecular vibration (RIV) of **Pt1**. However, the multiple intermolecular interactions of **Pt2** including C—H...F hydrogen bonding, Pt...Pt interactions and C—H... π intermolecular interaction, restrict both the intramolecular rotation (RIR) and vibration (RIV), resulting in a more rigid molecular environment to suppress the non-radiative process. The TEM images illustrate that regular square nanosheets are observed with different sizes from **Pt2** in CH₂Cl₂/n-hexane. This work represents the control of the luminescence properties of the neutral platinum(II) complexes by constructing intermolecular interactions, which may open up a new concept for the design of AIPE-active platinum(II) complexes rationally.

Experimental section

Experimental details, synthetic procedures, characterization and other experimental data are listed in the supporting information, including Schemes S1–S2, Tables S1–S4 and Fig. S1–Fig. S8.

Declaration of Competing Interest

The authors declare that they have no known competing financial interests or personal relationships that could have appeared to influence the work reported in this paper.

Acknowledgements

The authors thank the financial support from the National Natural Science Foundation of China (21978042, 21421005), and Talent Fund of Shandong Collaborative Innovation Center of Eco-Chemical Engineering (XTCXYX02).

Appendix A. Supplementary data

Supplementary data to this article can be found online at <https://doi.org/10.1016/j.tetlet.2020.152802>.

References

- [1] V.-W.-W. Yam, K.-M.-C. Wong, *Chem. Commun.* 47 (2011) 11579–11592.
- [2] V.-W.-W. Yam, K.-H.-Y. Chan, K.-M.-C. Wong, B.-W.-K. Chu, *Angew. Chem., Int. Ed.* 45 (2006) 6169–6173.
- [3] N. Liu, Y. Wang, C. Wang, Q. He, W. Bu, *Macromolecules* 50 (2017) 2825–2837.
- [4] F. Qu, B. Yang, Q. He, W. Bu, *Polym. Chem.* 8 (2017) 4716–4728.
- [5] W. Meng, Q. He, M. Yu, Y. Zhou, C. Wang, B. Yu, B. Zhang, W. Bu, *Polym. Chem.* 10 (2019) 4477–4484.
- [6] W. Meng, X. Qiu, R. Wang, Q. He, W. Bu, *J. Mater. Chem. C* 8 (2020) 15616–15621.
- [7] V.H. Houlding, V.M. Miskowski, *Coord. Chem. Rev.* 111 (1991) 145–152.
- [8] V.-W.-W. Yam, K.-M.-C. Wong, N. Zhu, *J. Am. Chem. Soc.* 124 (2002) 6506–6507.
- [9] W.-Y. Wong, G.-J. Zhou, X.-M. Yu, H.-S. Kwok, B.-Z. Tang, *Adv. Funct. Mater.* 16 (2006) 838–846.
- [10] S.S. Pasha, P. Das, N.P. Rath, D. Bandyopadhyay, N.R. Jana, I.R. Laskar, *Inorg. Chem. Commun.* 67 (2016) 107–111.
- [11] W.-C. Chen, C. Sukpattanacharoen, W.-H. Chan, C.-C. Huang, H.-F. Hsu, D. Shen, W.-Y. Hung, N. Kungwan, D. Escudero, C.-S. Lee, Y. Chi, *Adv. Funct. Mater.* (2020) 2002494.
- [12] K. Li, Q. Wan, C. Yang, X.-Y. Chang, K.-H. Low, C.-M. Che, *Angew. Chem., Int. Ed.* 57 (2018) 14129–14133.
- [13] X. Yang, H. Guo, X. Xu, Y. Sun, G. Zhou, W. Ma, Z. Wu, *Adv. Sci.* 6 (2019) 1801930.
- [14] X. Yang, L. Yue, Y. Yu, B. Liu, J. Dang, Y. Sun, G. Zhou, Z. Wu, W.-Y. Wong, *Adv. Opt. Mater.* (2020) 2000079.
- [15] G. Li, X. Zhao, T. Fleetham, Q. Chen, F. Zhan, J. Zheng, Y.-F. Yang, W. Lou, Y. Yang, K. Fang, Z. Shao, Q. Zhang, Y. She, *Chem. Mater.* 32 (2020) 537–548.
- [16] H.L. Steel, S.L. Allinson, J. Andre, M.P. Coogan, J.A. Platts, *Chem. Commun.* 51 (2015) 11441–11444.
- [17] S. Lin, H. Pan, L. Li, R. Liao, S. Yu, Q. Zhao, H. Sun, W. Huang, *J. Mater. Chem. C* 7 (2019) 7893–7899.
- [18] V.-W.-W. Yam, A.-S.-Y. Law, *Coord. Chem. Rev.* 414 (2020) 213298.
- [19] H. Xiao, L. Yan, E.M. Dempsey, W. Song, R. Qi, W. Li, Y. Huang, X. Jing, D. Zhou, J. Ding, X. Chen, *Prog. Polym. Sci.* 87 (2018) 70–106.
- [20] C. Chen, C. Gao, Z. Yuan, Y. Jiang, *Chin. Chem. Lett.* 30 (2019) 243–246.
- [21] I.B. Lozada, B. Huang, M. Stilgenbauer, T. Beach, Z. Qiu, Y. Zheng, D.E. Herbert, *Dalton Trans.* 49 (2020) 6557–6560.
- [22] Z. He, Y. Gao, H. Zhang, X. Wang, F. Meng, L. Luo, B.Z. Tang, *Chem. Commun.* 56 (2020) 7785–7788.
- [23] M.J.R. Thom, M.V. Babak, W.H. Ang, *Angew. Chem., Int. Ed.* 59 (2020) 2–10.
- [24] S.A. Jenekhe, J.A. Osahenu, *Science* 265 (1994) 765–768.
- [25] C. Wu, H. Peng, Y. Jiang, J. McNeill, *J. Phys. Chem. C* 110 (2006) 14148–14154.
- [26] J. Luo, Z. Xie, J.W.Y. Lam, L. Cheng, H. Chen, C. Qiu, H.S. Kwok, X. Zhan, Y. Liu, D. Zhu, B.Z. Tang, *Chem. Commun.* 18 (2001) 1740–1741.
- [27] G. Wei, Y. Jiang, F. Wang, *Tetrahedron Lett.* 59 (2018) 1476–1479.
- [28] S. Chen, R. Qiu, Q. Yu, X. Zhang, M. Wei, Z. Dai, *Tetrahedron Lett.* 59 (2018) 2671–2678.
- [29] L. Biesen, N. Nirmalanathan-Budau, K. Hoffmann, U. Resch-Genger, T.J.J. Müller, *Angew. Chem., Int. Ed.* 59 (2020) 10037–10041.
- [30] C. Zhang, R. Gao, H. Wang, S. Cheng, A. Xie, W. Dong, *Tetrahedron Lett.* 61 (2020) 152445.
- [31] J. Zhang, B. He, W. Wu, P. Alam, H. Zhang, J. Gong, F. Song, Z. Wang, H.H.Y. Sung, I.D. Williams, Z. Wang, J.W.Y. Lam, B.Z. Tang, *J. Am. Chem. Soc.* 142 (2020) 14608–14618.
- [32] T. Xiao, L. Zhou, X.-Q. Sun, F. Huang, C. Lin, L. Wang, *Chin. Chem. Lett.* 31 (2020) 1–9.
- [33] H. Honda, Y. Ogawa, J. Kuwabara, T. Kanbara, *Eur. J. Inorg. Chem.* (2014) 1865–1869.
- [34] J. Kuwabara, K. Yamaguchi, K. Yamawaki, T. Yasuda, Y. Nishimura, T. Kanbara, *Inorg. Chem.* 56 (2017) 8726–8729.
- [35] Y. Chen, C. Liu, L. Wang, *Tetrahedron* 75 (2019) 130686.
- [36] L. Wang, Z. Gao, C. Liu, X. Jin, *Mater. Chem. Front.* 3 (2019) 1593–1600.
- [37] Y. Xing, L. Wang, C. Liu, X. Jin, *Sens. Actuators, B* 304 (2020) 127378.
- [38] C. Liu, X. Song, X. Rao, Y. Xing, Z. Wang, J. Zhao, J. Qiu, *Dyes Pigm.* 101 (2014) 85–92.
- [39] Y. Xing, C. Liu, X. Song, J. Li, *J. Mater. Chem. C* 3 (2015) 2166–2174.
- [40] S. Tian, H. Ma, X. Wang, A. Lv, H. Shi, Y. Geng, J. Li, F. Liang, Z.-M. Su, Z. An, W. Huang, *Angew. Chem., Int. Ed.* 58 (2019) 6645–6649.
- [41] J. Mei, N.L.C. Leung, R.T.K. Kwok, J.W.Y. Lam, B.Z. Tang, *Chem. Rev.* 115 (2015) 11718–11940.
- [42] W.A. Ogden, S. Ghosh, M.J. Bruzek, K.A. McGarry, L. Balhorn, V. Young Jr., L.J. Purvis, S.E. Wegwerth, Z. Zhang, N.A. Serratore, C.J. Cramer, L. Gagliardi, C.J. Douglas, *Cryst. Growth Des.* 17 (2017) 643–658.
- [43] J. Guan, R. Wei, A. Prlj, J. Peng, K.-H. Lin, J. Liu, H. Han, C. Corminboeuf, D. Zhao, Z. Yu, J. Zheng, *Angew. Chem., Int. Ed.* 59 (2020) 2–9.
- [44] J. Mei, Y. Hong, J.W.Y. Lam, A. Qin, Y. Tang, B.Z. Tang, *Adv. Mater.* 26 (2014) 5429–5479.
- [45] Y. Hong, J.W.Y. Lam, B.Z. Tang, *Chem. Soc. Rev.* 40 (2011) 5361–5388.